

Supplementary Materials

The EGFR-TMEM167A-p53 Axis Defines the Aggressiveness of Gliomas

Berta Segura-Collar, Ricardo Gargini, Elena Tovar-Ambel, Esther Hernández-SanMiguel, Carolina Epifano, Ignacio Pérez de Castro, Aurelio Hernández-Laín, Sergio Casas-Tintó and Pilar Sánchez-Gómez

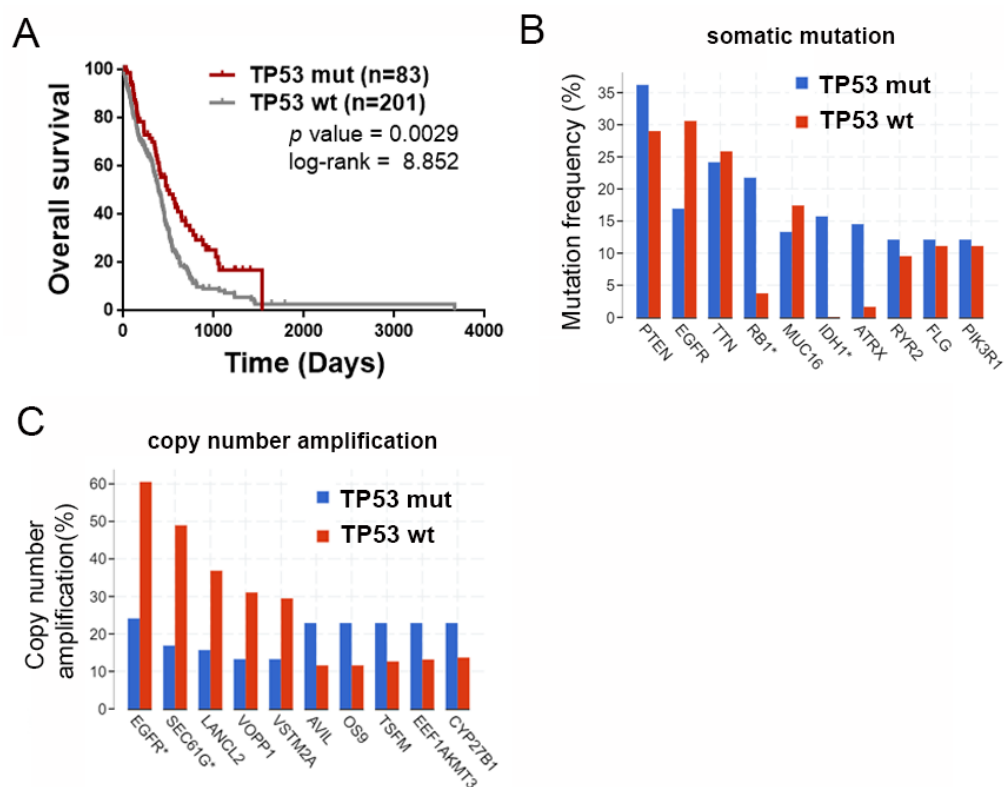


Figure S1. *TP53* opposes *EGFR* in glioblastoma. (A) Kaplan–Meier overall survival curves of patients from the TCGA LGG + GBM cohort. Patients were separated based on the *TP53* status. (B,C) Frequency analysis of somatic mutations (B) and copy number amplification (C) in glioblastomas grouped according to *TP53* status. * Statistically significant $p < 0.0001$.

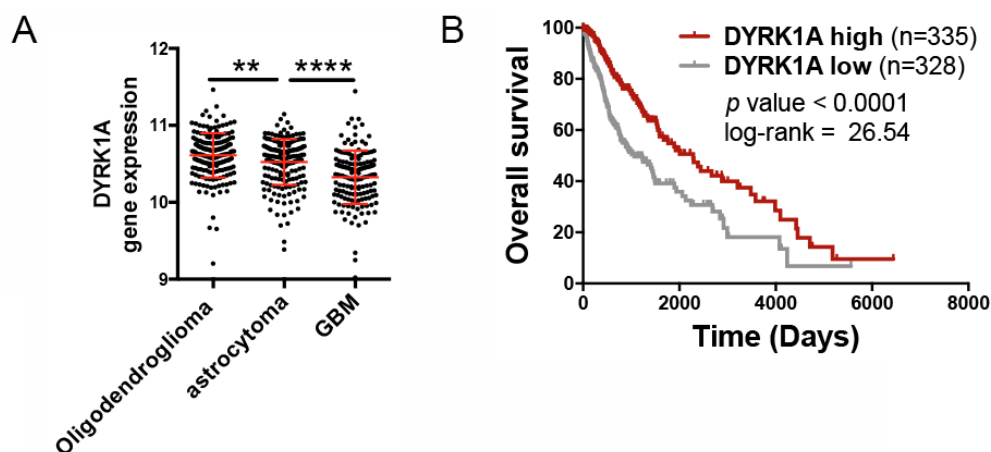


Figure S2. Expression and implication of *DYRK1A* in the pathology of gliomas. (A) Expression of *DYRK1A* in gliomas, grouped according to the histological type. (B) Kaplan–Meier overall survival

curves of patients from the TCGA LGG + GBM cohort. Patients were separated based on high and low *DYRK1A* expression values. ** $p \leq 0.01$; **** $p \leq 0.0001$.

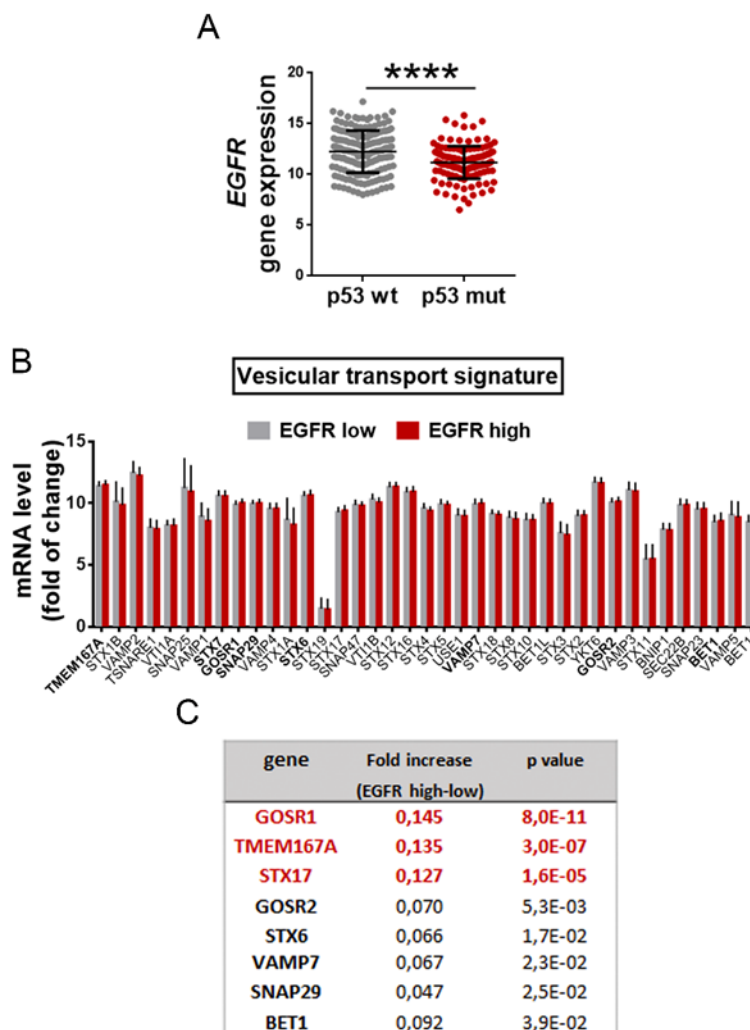


Figure S3. Vesicular transport genes associated to *EGFR* in gliomas. (A) Levels of *EGFR* mRNA measured by RNAseq in gliomas (LGG + GBM TCGA cohort), comparing wild-type and mutant *TP53* tumors. (B,C) Vesicular transport signature in gliomas of the TCGA (LGG + GB cohort). Tumors were classified based on high or low *EGFR* expression. **** $p \leq 0.0001$.

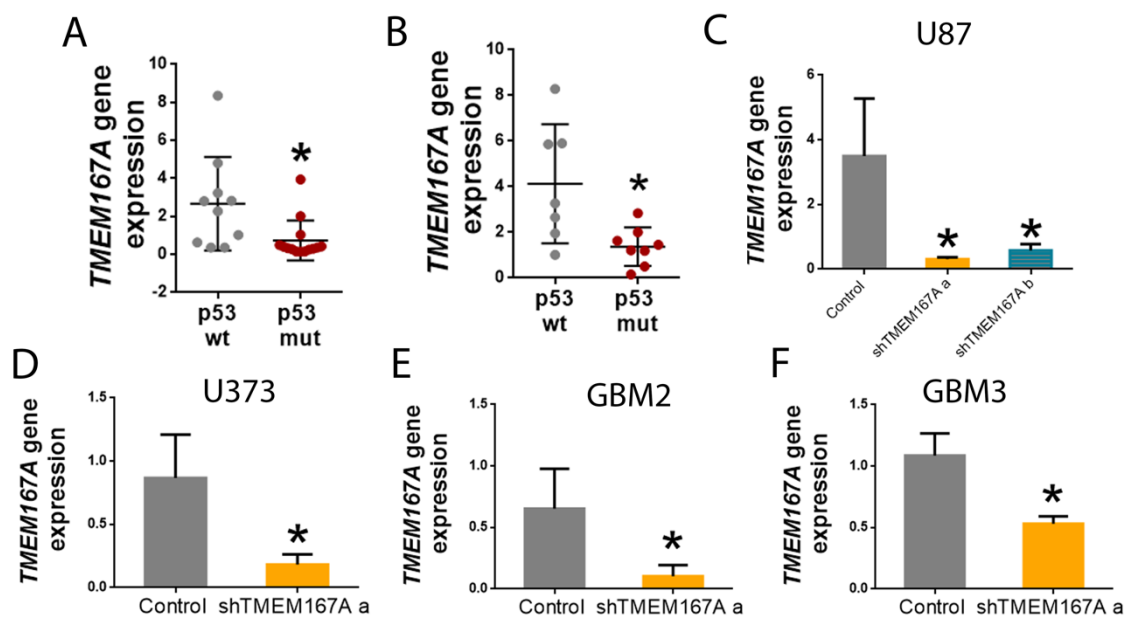


Figure S4. *TMEM167A* downregulation in subcutaneous tumor tissue. (A,B) qRT-PCR analysis of *TMEM167A* in our own cohort of glioma samples. Patients (A) and PDXs (B) were stratified based on TP53 status: p53 wt and p53 mut. *HPRT* was used for normalization. (C-F) *TMEM167A* levels were determined by qRT-PCR in U87 (A), U373 (B), GBM2 (C), and GBM3 (D) tumor tissue (control, shTMEM167Aa, or shTMEM167Ab). *HPRT* was used for normalization. * $p \leq 0.05$.

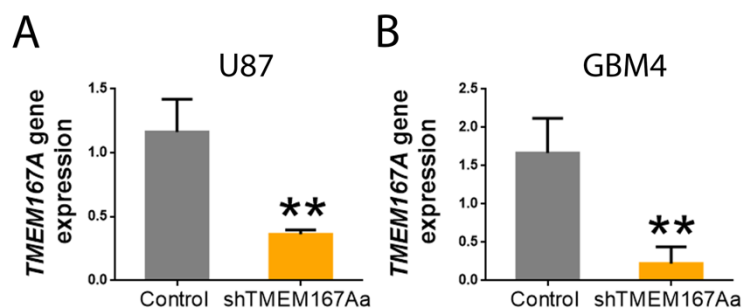


Figure S5. Downregulation of *TMEM167A* in intracranial tumors. (A,B) *TMEM167A* expression was determined by qRT-PCR in U87 (A) and U373 (B) tumor tissue (control or shTMEM167Aa). ** $p \leq 0.01$.

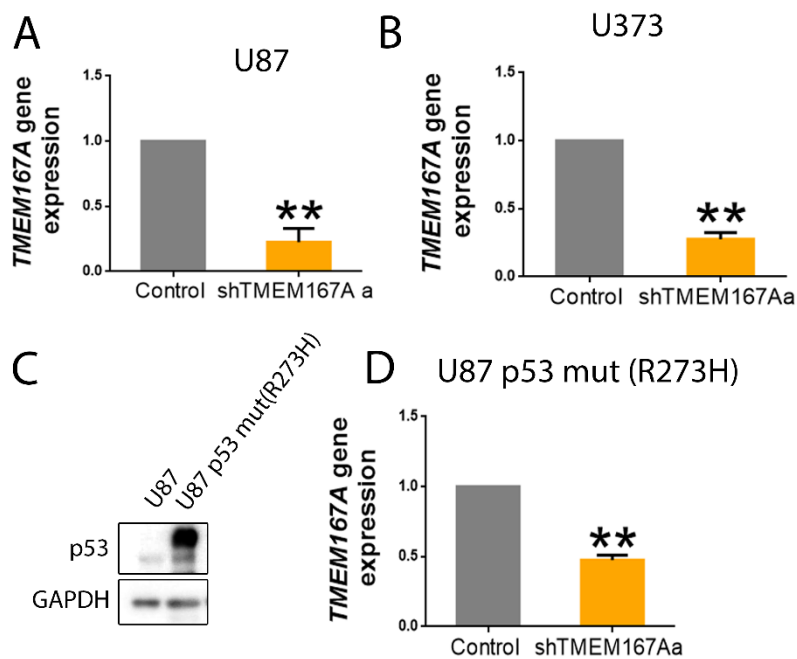


Figure S6. Downregulation of *TMEM167A* in cultured GBM cells. (A,B) *TMEM167A* levels were determined by qRT-PCR in U87 (A) and U373 (B) cells (control or sh*TMEM167Aa*). *HPRT* was used for normalization. (C) WB analysis of p53 in U87 and U87 p53 mut (R273H) cells. GAPDH was used as a loading control. (D) *TMEM167A* levels were determined by qRT-PCR in U87 p53 mut (R273H) cells (control or sh*TMEM167Aa*). ** $p \leq 0.01$.

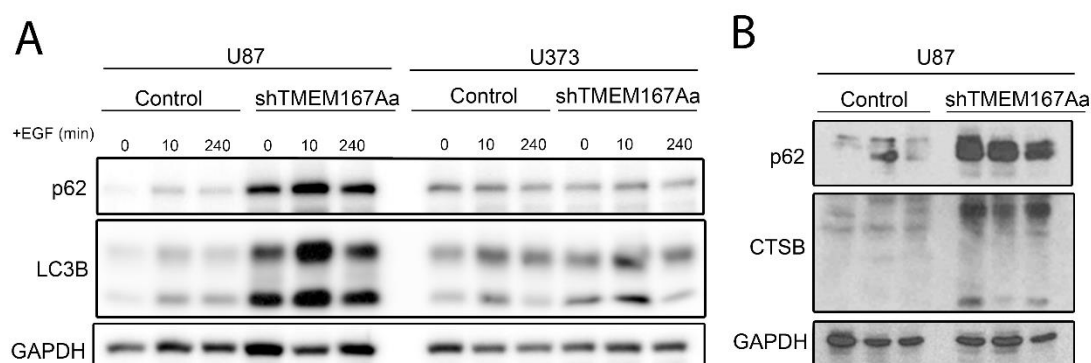


Figure S7. Analysis of autophagy-related proteins after *TMEM167A* downregulation. (A) Growth-factor-starved U87 and U373 cells (Control or sh*TMEM167Aa*) were stimulated with 100 ng/mL of EGF for the indicated times; p62 and LC3B were tested by WB; GAPDH was used as loading control. (B) WB analysis of p62 and Cathepsin B (CTSB) in tumors from Figure 5A. GAPDH was used as a loading control.

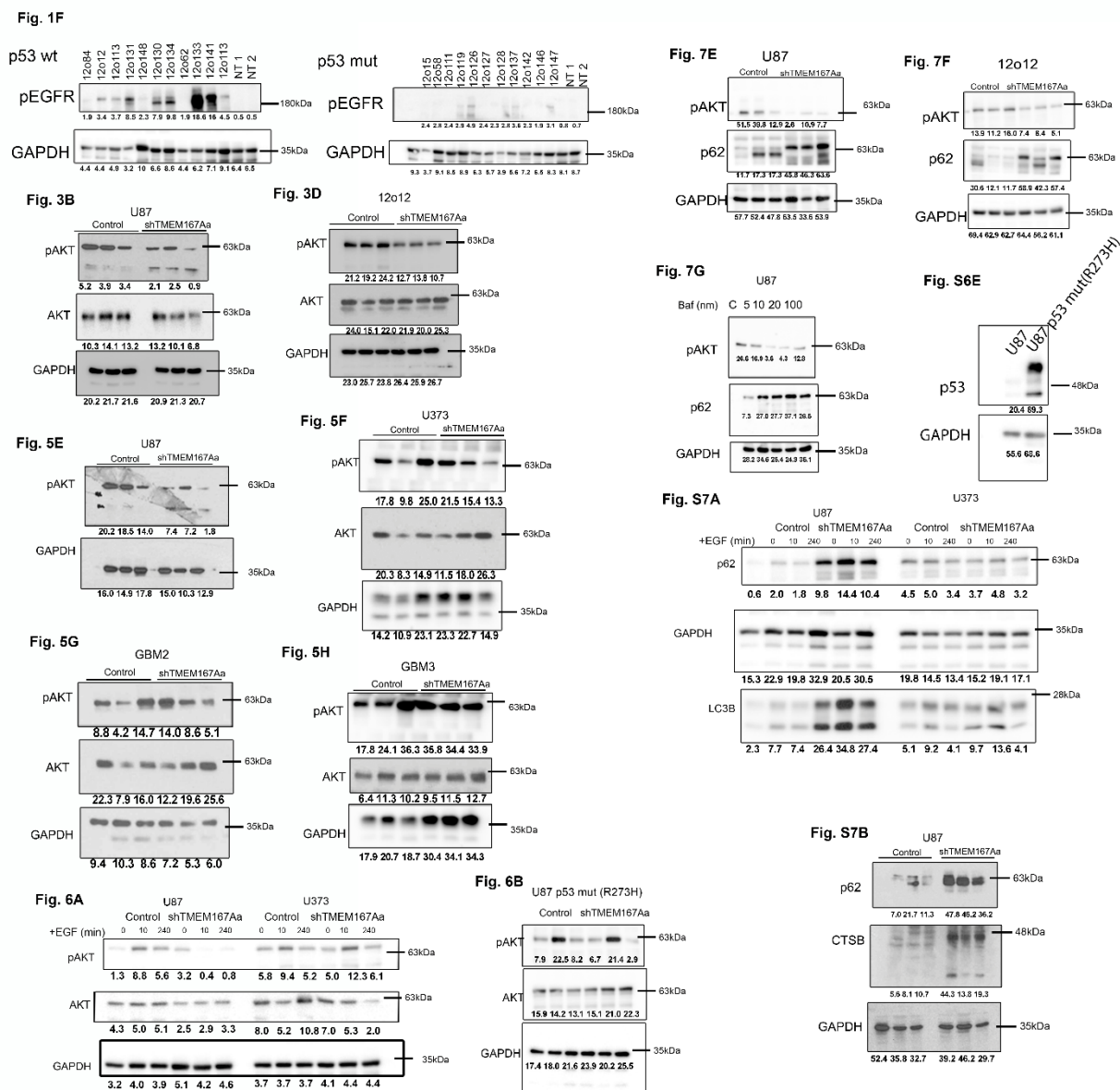


Figure S8. Full scan of the different WBs.

Table S1. Human samples (n.d. = not diagnosed; wt = wild type; and mut = mutated).

Sample (12o)	Diagnosis	IDH	EGFR	Tp53
1	GBM	n.d.	mut(vIII)	mut
7	GBM	wt	amp	mut
9	GBM	n.d.	wt	mut
10	GBM	n.d.	n.d.	n.d.
11	GBM	n.d.	n.d.	n.d.
12	GBM	wt	mut(vIII)	wt
14	GBM	n.d.	n.d.	n.d.
15	GBM	wt	wt	mut
16	GBM	wt	n.d.	wt
17	GBM	n.d.	wt	n.d.
18	GBM	n.d.	wt	n.d.
21	GBM	mut	wt	mut
23	GBM	wt	amp	wt
26	GBM	n.d.	n.d.	n.d.
27	GBM	wt	wt	mut
42	GBM	n.d.	n.d.	n.d.
45	GBM	n.d.	n.d.	n.d.
46	GBM	n.d.	n.d.	n.d.
48	GBM	n.d.	n.d.	n.d.
49	GBM	n.d.	n.d.	n.d.
52	GBM	n.d.	n.d.	n.d.
58	GBM	wt	wt	mut
59	GBM	n.d.	n.d.	n.d.
60	GBM	n.d.	n.d.	n.d.
62	GBM	wt	n.d.	wt
70	GBM	wt	mut	n.d.
72	GBM	n.d.	n.d.	n.d.
73	GBM	wt	wt	wt
74	GBM	wt	wt	wt
76	GBM	wt	amp	wt
77	GBM	wt	wt	wt
84	GBM	wt	mut	wt
97	GBM	wt	amp	wt
107	GBM	wt	wt	n.d.
108	GBM	wt	wt	n.d.
111	GBM	n.d.	n.d.	mut
113	GBM	wt	amp	wt
116	GBM	mut	wt	mut
117	GBM	n.d.	n.d.	n.d.
118	GBM	n.d.	n.d.	n.d.
119	GBM	n.d.	n.d.	mut
121	GBM	wt	amp	n.d.
122	GBM	wt	n.d.	n.d.
124	GBM	wt	n.d.	n.d.
126	GBM	wt	n.d.	mut
127	GBM	n.d.	n.d.	mut
128	GBM	n.d.	n.d.	mut
129	GBM	n.d.	wt	mut
130	GBM	n.d.	n.d.	wt
131	GBM	wt	mut	wt
133	GBM	n.d.	n.d.	wt
134	GBM	n.d.	n.d.	wt
137	GBM	n.d.	n.d.	mut
141	GBM	n.d.	n.d.	wt
142	GBM	n.d.	n.d.	mut
146	GBM	n.d.	n.d.	mut
147	GBM	n.d.	n.d.	mut
148	GBM	n.d.	n.d.	wt
149	GBM	wt	wt	n.d.



© 2020 by the authors. Licensee MDPI, Basel, Switzerland. This article is an open access article distributed under the terms and conditions of the Creative Commons Attribution (CC BY) license (<http://creativecommons.org/licenses/by/4.0/>).